



# Structural connectivity and weight loss in children with obesity: a study of the “connectobese”

Mireille J. C. M. Augustijn<sup>1,2</sup> · Maria A. Di Biase<sup>3,4,5</sup> · Andrew Zalesky<sup>3,4,6</sup> · Lore Van Acker<sup>7</sup> · Ann De Guchtenaere<sup>7</sup> · Eva D'Hondt<sup>8</sup> · Matthieu Lenoir<sup>1</sup> · Frederik J. A. Deconinck<sup>1</sup> · Karen Caeyenberghs<sup>9</sup>

Received: 19 March 2018 / Revised: 1 April 2019 / Accepted: 7 April 2019 / Published online: 26 July 2019  
© The Author(s), under exclusive licence to Springer Nature Limited 2019

## Abstract

**Background** Previous studies suggest that obesity (OB) is associated with disrupted brain network organization; however, it remains unclear whether these differences already exist during childhood. Moreover, it should be investigated whether deviant network organization may be susceptible to treatment.

**Methods** Here, we compared the structural connectomes of children with OB with age-matched healthy weight (HW) controls (aged 7–11 years). In addition, we examined the effect of a multidisciplinary treatment program, consisting of diet restriction, cognitive behavioral therapy, and physical activity for children with OB on brain network organization. After stringent quality assessment criteria, 40 (18 OB, 22 HW) data sets of the total sample of 51 participants (25 OB, 26 HW) were included in further analyses. For all participants, anthropometric measurements were administered twice, with a 5-month interval between pre- and post tests. Pre- and post T1- and diffusion-weighted imaging scans were also acquired and analyzed using a graph-theoretical approach and network-based statistics.

**Results** Global network analyses revealed a significantly increased normalized clustering coefficient and small-worldness in children with OB compared with HW controls. In addition, regional analyses revealed increased betweenness centrality, reduced clustering coefficient, and increased structural network strength in children with OB, mainly in the motor cortex and reward network. Importantly, children with OB lost a considerable amount of their body mass after the treatment; however, no changes were observed in the organization of their brain networks.

**Conclusion** This is the first study showing disrupted structural connectomes of children with OB, especially in the motor and reward network. These results provide new insights into the pathophysiology underlying childhood obesity. The treatment did result in a significant weight loss, which was however not associated with alterations in the brain networks. These findings call for larger samples to examine the impact of short-term and long-term weight loss (treatment) on children's brain network organization.

## Introduction

Childhood obesity (OB) is a challenging threat to global health, because it is often associated with other health

diseases, such as type 2 diabetes and cardiovascular diseases [1, 2]. Excessive eating behavior and reduced levels of physical activity have shown to be the main causes of this multifactorial health problem [1, 3, 4], and weight loss programs are recommended to be multidisciplinary with focus on eating and exercise behavior. Optimal regulation of these behaviors relies on an integrated and efficient information processing of the brain network [5, 6]. For example, in a daily life context, the individual is challenged to ignore or inhibit unhealthy stimuli (e.g., eating a chocolate bar) that would instantly trigger the reward center and instead opt for the less “rewarding” bout of physical activity [7]. Previous neuroimaging studies suggest that childhood OB is associated with differences in gray matter density [8, 9] and white matter organization [8, 10], mainly in

---

These authors contributed equally as joint seniors: Frederik J. A. Deconinck, Karen Caeyenberghs

---

**Supplementary information** The online version of this article (<https://doi.org/10.1038/s41366-019-0380-6>) contains supplementary material, which is available to authorized users.

---

✉ Mireille J. C. M. Augustijn  
[mireille.augustijn@ugent.be](mailto:mireille.augustijn@ugent.be)

Extended author information available on the last page of the article.

frontal and temporal brain regions. Moreover, previous work from our lab has shown that a multidisciplinary treatment program at the Zeepreventorium (De Haan, Belgium) resulted in a significant increase in total and cerebellar gray matter volume in children with OB, while no change was observed in the healthy weight (HW) controls [11]. These findings indicate that typical unhealthy behavior in individuals with OB indeed may be related to altered brain structures in specific regions. Nevertheless, to understand the impact of childhood OB on the global organization of brain networks, it is important to move beyond isolated brain regions and evaluate the brain as a large-scale network [12].

Graph theory is a mathematical framework which represents the brain as a connectome consisting of nodes (i.e., brain regions) and edges (i.e., functional or structural connections between brain regions) [13]. Graph metrics can be calculated to identify highly efficient brain networks, known as small-world networks, which are characterized by high local segregation (i.e., dense local clustering between neighboring nodes) and high global integration (i.e., short path lengths between any pair of nodes) [14]. Graph theory enables to quantify interactions between brain regions, rather than assuming that brain areas act as independent processors. In this way, graph metrics can provide complementary characterization of brain development in childhood OB and related behaviours [12, 15, 16]. Moreover, graph theory has been useful for detecting disease-related differences and alterations in brain network organization across a wide range of clinical populations (see Griffa et al. [17] for a review).

To date, only a few studies have used graph theory to examine brain network organization in relation to OB, albeit in adults. Chao et al. [18] and Baek et al. [19], for example, observed reduced small-world characteristics in brain networks of adults with OB ( $N_{\text{Chao}} = 20/N_{\text{Baek}} = 40$ ; 22–58 years old) compared with HW controls, using resting-state functional magnetic resonance imaging (MRI). Specifically, OB was associated with reduced local segregation characterized by a lower normalized clustering coefficient and altered (i.e., increased or decreased) global integration characterized by a lower global efficiency, and normalized characteristic path length in the global brain network. In addition, network-based statistics (NBS) (i.e., edgewise comparisons) revealed a decreased functional network strength (i.e., lower functional connectivity) in the corticostriatal/cortico-thalamic network of adults with OB [19]. Finally, a diffusion MRI study showed reduced (structural) node strength (i.e., sum of the weights of all the edges connected to each node) and normalized the clustering coefficient (i.e., segregation) in subjects with OB ( $N = 31$ , 12–39 years old) compared with HW controls, with more pronounced results in the reward network [20]. Altogether,

these studies suggest that OB is associated with an imbalance between local segregation and global integration, and disrupted networks, which may lead to less efficient information processing in the brain network. However, it remains unclear whether these network differences also exist in (young) children with OB, because graph theory studies in relation to OB have only focused on adolescents and adults so far. Moreover, no research is available on the effect of a specialized multidisciplinary weight reduction OB program on structural brain connectivity and network organization. As previous neuroimaging studies in other clinical populations (such as traumatic brain injury) have shown that graph metrics and structural network strength show promising validity as “biomarkers” to examine training-induced alterations [21–25], examining the effect of multidisciplinary treatment on structural brain connectivity and network organization in children with OB can provide greater insight into the structural neuroplasticity underlying weight loss.

Therefore, this study set out to examine global and regional brain network properties in children with OB, using graph-theoretical analysis (i.e., graph metrics; node-wise comparisons) and NBS (i.e., structural network strength; edgewise comparisons) [26]. Our first aim was to compare structural segregation, global integration, and structural network strength between children with OB and HW controls. The second aim of this study was to determine the effect of a specialized multidisciplinary weight reduction OB program on structural brain connectivity and network organization. Based on previous studies in adults with OB [18–20], we expected that children with OB would display a reduced clustering coefficient, characteristic path length, and small-worldness compared with HW controls and that these alterations would resolve following treatment. At the regional level, significant differences in brain network organization were expected to be most pronounced in the reward network.

## Methods

### Participants

Fifty-one children (20 girls,  $9.5 \pm 1.0$  years, range 7.8–11.6 years) participated in this study. The children with OB ( $N = 25$ , 12 girls,  $9.6 \pm 0.9$  years) were recruited via a local rehabilitation center, where they attended a multidisciplinary OB program. This group of children was classified as obese according to the internationally accepted age-specific and sex-specific cutoff points for children [27]. An age-matched (i.e., within 6 months) control group ( $N = 26$ , 8 girls,  $9.5 \pm 1.1$  years) was recruited through local primary schools. These participants were classified as HW

according to the same cutoff points and were not involved in any kind of treatment during the course of the study (see Fig. S1 in Supplemental Material 1 for an overview of the study sample). The protocol of the study was approved by the Ethical Committee of the Ghent University Hospital prior to data collection. The children and their parent(s) or legal caretaker(s) were fully informed about the study, and parents always discussed with their child if they were willing to participate, before signing the informed consent.

## Procedure

All participants were assessed on two occasions with a 5-month time interval between the pre test and post test (OB:  $147 \pm 21$  days; HW:  $154 \pm 12$  days). For the children with OB, measurements at the pretest were taken at the start of the multidisciplinary OB program. A detailed description of the program can be found in our previous work [28, 29]. Briefly, children with OB followed a multidisciplinary OB program at the rehabilitation center Zeepreventorium (De Haan, Belgium). During the treatment, children were full-time residents at the center and only went home (i.e., three times a month) during weekends. The program focused on three central pillars, including moderate diet restriction, cognitive behavioral therapy, and regular physical activity. The duration of the treatment program was 10 months in total; however, previous studies from our lab observed a considerable amount of

weight loss after only 4 months of treatment with the Zeepreventorium (i.e., 11.7 kg/17.9% on average; 28, 29). This weight loss was further accompanied by significant improvements in children's gross and fine motor competence. These findings, in combination with methodological (e.g., stability of the scanner) and practical issues (e.g., minimizing the dropout rate, planning with the rehabilitation center), motivated our decision to select a 5-month time interval between pre-measurement (i.e., prior to the start of the treatment program) and post-measurement.

## MRI acquisition

In this study, T1-weighted and diffusion-weighted images were acquired on a 3T Siemens Magnetom Trio MRI scanner system (Siemens, Erlangen, Germany). All MRI analyses were performed on the high-performance computing infrastructure of Multi-modal Australian ScienceS Imaging and Visualization Environment (MASSIVE) [30]. An overview of the processing pipeline is shown in Fig. 1. Refer to Supplemental Material 2 for acquisition parameters, preprocessing, and tractography pipeline.

## Network construction

Connectivity matrices were weighted by the number of reconstructed streamlines (NOS), which represents the total

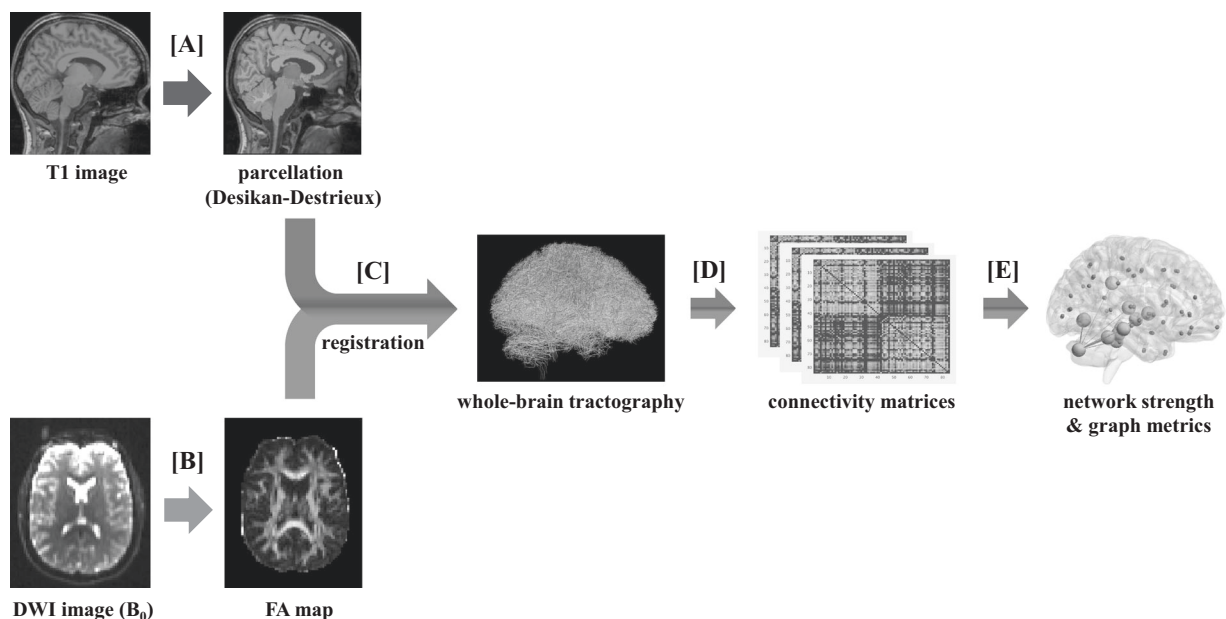


**Fig. 1** Overview of the processing pipeline. **a** and **b** First, the T1 image and diffusion-weighted images (DWI) were preprocessed using FreeSurfer (<http://surfer.nmr.mgh.harvard.edu>) and FSL [62]. **c** Second, the T1-weighted images were registered to the FA map and then automated whole-brain tractography was performed using MRtrix3 [63]. **d** Symmetric  $N \times N$  connectivity matrices were generated for

each subject and each time point, whereby  $N$  represents 84 cortical and subcortical (including the cerebellum) regions (i.e., nodes) of the Desikan–Killiany atlas [64]. **e** The network strength (structural) and graph metrics were calculated and compared between groups (cross-sectional) and across time points (longitudinal)

number of interregional connections (i.e., edges) between each pair of nodes. These NOS were calculated using a probabilistic tractography algorithm, which can improve sensitivity (i.e., low number of false negatives), but often results in spurious connections known as false positives and yields almost fully connected matrices with a connection density of  $\sim 0.9$ – $0.95$  [31, 32]. Since fully connected structural networks are more than likely nonbiological plausible (i.e., connection density  $> 0.5$ ) [31, 33], the following thresholding procedure was applied to eliminate spurious and discarded connections: (i) on the one hand, an edge was set to zero for connections with NOS lower than  $k$  (here:  $k = 115$ ), whereby  $k$  was the lowest NOS for which the highest connection density did not exceed 0.5 [34] and the lowest connection density did not result in fragmented networks; (ii) on the other hand, a group threshold of 60% was applied across all subjects and all time points, whereby a connection needed to be present in at least 60% of the subjects across time points to be included [35]. This resulted in a mean connection density of 0.4. Since results can differ across connection densities, this thresholding procedure was repeated using group thresholds ranging from 30% to 90% (interval 15%) to check the robustness of the results (density range:  $\sim 0.3$ – $0.5$ ).

### Anthropometric measurements

Body height (0.1 cm, Harpenden, Holtain, Ltd., Crymch, UK), body weight (0.1 kg), and fat percentage (0.1%, Tanita, BC420SMA, Weda B.V., Naarden, Holland) were assessed in minimal clothing on the day of the MRI scanning. Children were classified as being HW or obese by calculating the body mass index (BMI,  $\text{kg}/\text{m}^2$ ) [27]. In addition, children's waist circumference (0.1 cm) was measured using a flexible tape measure. Socioeconomic status was self-assessed by the parents based on family income level. In a pediatric sample, there may be a great variation in maturity, which also affects brain development. To control for these maturity effects, Tanner staging for puberty was self-assessed by the children and their parents, based on breast development in girls (stage 1–5) and testicular size in boys (stage 1–5) [36].

### Statistical analyses

#### Network-based statistical analysis

The NBS toolbox version 1.2 [26] was used to (i) test for group differences in structural network strength at the pretest; and (ii) test for time by group interaction effects in connectivity strength of the structural brain networks. The NBS toolbox is a validated method to deal with the multiple comparisons problem by using a nonparametric statistical

approach [26]. The following multistep procedure was performed: first, the hypothesis of interest was tested with a single univariate test statistic for every connection in the network. Second, a test statistic threshold was determined, whereby a test statistic value exceeding the threshold of  $t = 2.5$ , 3, and 3.5 was admitted to a set of suprathreshold connections. Third, connected components (i.e., subnetworks) were identified, whereby a component was defined as a group of suprathreshold connections for which a path can be found between any pair of nodes. Finally, a  $p$ -value was computed for each connected component, using permutation testing (i.e., 5000 permutations) with a familywise error rate (FWE) correction for multiple comparisons. For each permutation testing, data of all subjects were randomly assigned to the group of OB or HW. In addition to the NBS analyses, repeated measures ANOVA (time by group interaction effect) was performed to compare the global network strength (i.e., total NOS; structural) between groups and across time points. For all the analyses, age was included as a nuisance covariate.

#### Graph-theoretical network analysis

Complementary to NBS analyses (i.e., edgewise comparison), network properties were compared using the cross-sectional batch (group differences) and longitudinal pipeline (time by group interaction effects) of the graph analysis toolbox (GAT) [34]. First, 20 null networks were generated for network normalization by comparing each edge weight with the mean edge weight across the network. Then, the following graph metrics were extracted using the brain connectivity toolbox [13]: normalized characteristic path length, normalized clustering coefficient, and small-worldness (see Table 1 for a detailed description of these graph metrics). Subsequently, a nonparametric permutation test with 5000 repetitions was used to test for statistically significant between-group differences (in changes) of graph metrics (slope). For each permutation, regional data of each participant (at both time points) were randomly allocated to one of two groups, with the same number of subjects as the initial groups. The differences in slope between randomized groups were then calculated and compared with the actual differences in the slope between the original groups to obtain a  $p$ -value. The same permutation procedure was applied to test for regional differences in the clustering coefficient. For these regional analyses, the false discovery rate or FDR-corrected  $p$ -values were obtained to control for multiple comparisons. The significance threshold was set at  $p < 0.05$ . Finally, network hubs, which are the most important regions in the brain, were defined based on betweenness centrality (mean + two standard deviations). Since the longitudinal plugin of the GAT toolbox does not include network hub analysis, the network hubs were only

**Table 1** Description of graph metrics

Measure	Description
Connection density	The proportion of possible connections in the brain network that are actual connections (number of connections/total number of possible connections)
Global network strength	Level of connectivity (defined here as the number of reconstructed streamlines) of the entire brain network
Network strength	Level of connectivity (defined here as the number of reconstructed streamlines) between node $i$ and node $j$
<i>Measures of global integration</i>	
Clustering coefficient	The number of edges that exist between the nearest neighbors of a node proportionally to the maximum number of possible connections
Normalized clustering coefficient ( $\gamma$ )	The clustering coefficient was normalized by comparing this parameter with the mean clustering coefficient of 5000 random networks with the same density
<i>Measures of local segregation</i>	
Characteristic path length	Mean of shortest paths ( $L$ ) between all nodes in the network
Normalized characteristic path length ( $\lambda$ )	The characteristic path length was normalized by comparing this parameter with the mean path length of 5000 random networks with the same density
Betweenness centrality	The fraction of all shortest paths in the network that pass through a given node
Hubs (betweenness centrality)	Central and highly connected regions in the brain characterized by a betweenness centrality that is two standard deviations higher than the mean network betweenness centrality
<i>Small-world network</i>	
Small-worldness	Small-worldness ( $\sigma = \gamma/\lambda > 1$ ) was characterized by a high local interconnectivity of the nodes ( $\gamma \gg 1$ ) and an equivalent shortest path length ( $\lambda \approx 1$ ) compared with the random networks

identified at the pretest. To check the robustness of significant results across all group thresholds (30–90%), the area under the curve (AUC) was calculated by summing the value of the graph measures at each threshold. In addition, one-way and/or repeated measures ANCOVAs, with age as a covariate, were performed to test for between-group differences (in changes) of graph metrics across thresholds.

### Anthropometric measurements

Statistical analyses were performed using SPSS Statistics (Version 22.0). Before analysis, data were checked for normality. Changes in anthropometric measurements were evaluated using a 2 (group)  $\times$  2 (time) repeated measures ANOVA. In addition, partial correlations (controlling for age) were performed between (1) structural network strength or graph metrics and anthropometric measurements at the pretest; (2) structural network strength and/or graph metrics at the pretest and changes in weight-related measures ( $\frac{\text{post-pre}}{\text{post}} \times 100\%$ ); (3) changes in brain network strength (structural) and/or graph metrics (post–pre) and changes in weight-related measures. FDR corrections were made to control for multiple comparisons. The significance threshold was set at  $p < 0.05$ .

## Results

### Participants

From the initial sample of 25 children with OB, MRI data of seven participants (3 girls,  $9.9 \pm 0.8$ ) had to be excluded due to claustrophobia, scanner/motion artifacts, or low quality of the image registration. This resulted in a final OB sample of 18 children (9 girls,  $9.4 \pm 1.0$  years) with good-quality pre-MRI and post-MRI data. Of the 26 children with a HW, two children (1 girl,  $8.5 \pm 0.3$  years) dropped out during the course of the study and MRI data of two children (2 boys,  $9.1 \pm 0.4$ ) had to be excluded due to scanner artifacts or low quality of the image registration. This left us with a final control sample of 22 children with a HW (7 girls,  $9.6 \pm 1.2$  years). As shown in Table 2, children with OB had significantly lower socioeconomic status compared with HW controls. No significant group differences were observed for height, age, and pubertal status at the pretest ( $p > 0.05$ ).

### Network-based statistical analysis

At the pretest, the NBS ( $t = 3.5$ ) revealed a significantly higher connected subnetwork in children with OB

**Table 2** Descriptive statistics (mean  $\pm$  standard deviation) for the group of children with obesity and children with a healthy weight at the pre and post test (5-months' time interval between pre and post)

	Time 1 (pre)		Chi-square $\chi^2$	T-test <sup>a</sup> <i>t</i>	Time 2 (post)		Repeated measures ANOVA		
	OB ( <i>N</i> = 18)	HW ( <i>N</i> = 22)			OB ( <i>N</i> = 18)	HW ( <i>N</i> = 22)	<i>F</i> <sub>TIME</sub>	<i>F</i> <sub>GROUP</sub>	<i>F</i> <sub>TIME*GROUP</sub>
<i>Demographics</i>									
Sex	9♂, 9♀	15♂, 7♀	1.364		9♂, 9♀	15♂, 7♀			
Age (years)	9.5 $\pm$ 1.0	9.6 $\pm$ 1.2		-0.380	9.9 $\pm$ 1.0	10.0 $\pm$ 1.2	2 944.006**	0.164	1.336
<i>Pubertal status</i> <sup>b</sup>									
			2.129						
Stage 1	11 (61.2%)	18 (81.8%)							
Stage 2	4 (22.2%)	3 (13.6%)							
Stage 3	3 (16.7%)	1 (4.5%)							
Stage 4	0	0							
Stage 5	0	0							
<i>Income level (SES)</i>									
			11.810*						
Missing	1 (5.6%)	1 (4.5%)							
<20,000/year	7 (38.9%)	1 (4.5%)							
20,000–30,000/year	6 (33.3%)	4 (18.2%)							
>30,000/year	4 (22.2%)	16 (72.7%)							
<i>Anthropometric measurements</i>									
Body height (cm)	142.0 $\pm$ 6.8	139.9 $\pm$ 9.2		0.823	144.5 $\pm$ 7.3	142.8 $\pm$ 9.4	385.201**	0.533	2.281
Body weight (kg)	64.1 $\pm$ 11.3	33.3 $\pm$ 5.8		10.470**	53.7 $\pm$ 9.4	34.8 $\pm$ 6.1	129.699**	91.529**	236.554**
Body fat (%)	45.4 $\pm$ 6.0	17.6 $\pm$ 4.5		16.818**	33.6 $\pm$ 6.5	17.6 $\pm$ 4.2	83.121**	201.014**	85.077**
Total fat mass (kg)	29.3 $\pm$ 7.6	5.8 $\pm$ 1.7		12.833**	18.3 $\pm$ 6.3	6.2 $\pm$ 2.0	112.015**	148.369**	127.880**
Total fat-free mass (kg)	34.7 $\pm$ 5.8	27.5 $\pm$ 5.2		4.197**	35.4 $\pm$ 5.6	28.6 $\pm$ 5.0	13.973**	17.216**	1.100
Waist circumference (cm)	94.5 $\pm$ 8.4	61.3 $\pm$ 4.3		15.228**	82.1 $\pm$ 6.4	60.1 $\pm$ 8.8	264.211**	178.146**	277.096**
Body mass index (kg/m <sup>2</sup> )	31.64 $\pm$ 4.35	16.85 $\pm$ 1.15		14.030**	25.66 $\pm$ 3.68	16.93 $\pm$ 1.19	30.076**	208.810**	20.444**

OB obesity, HW healthy weight, SES socioeconomic status

\* $p < 0.05$ ; \*\* $p \leq 0.001$

<sup>a</sup>Independent sample *t*-test

<sup>b</sup>Tanner staging for puberty was based on breast development in girls (stage 1–5) and testicular size in boys (stage 1–5). For analysis purposes, stages 2–5 were combined into a larger group (0 = stage 1, 1 = stages 2–5)

compared with the HW control group ( $p = 0.046$ ; see Fig. S2 in Supplemental Material 3 for results with a *t*-statistic threshold of  $t = 3$  and  $t = 2.5$ ). Specifically, this subnetwork consisted of three edges connecting four nodes, including the right accumbens area, right putamen, and bilateral caudate (see Fig. 2b, c). This higher connected subnetwork remained significant for all group thresholds considered ( $p$ 's: 0.0354–0.0492, FWE-corrected), except for a group threshold of 30% ( $p = 0.0568$ ). The results from the longitudinal NBS analysis revealed no significant time by group interaction effects in structural network strength ( $p > 0.05$ ), indicating that the between-group difference in structural network strength did not change after OB treatment. In addition, the repeated measures ANOVA revealed that the total NOS did not differ between both groups across time points ( $p > 0.05$ ; see Fig. 2a). The analyses were repeated with sex as a fixed factor. No significant group by sex interaction effects was observed. We can tentatively

conclude that sex did not significantly influence the observed group differences in structural connectivity.

## Graph-theoretical network analysis

### Global network properties

Small-worldness ( $\sigma = \text{normalized clustering coefficient } (\gamma) / \text{normalized characteristic path length } (\lambda) > 1$ ) was observed in all children, indicating that all participants had high local interconnectivity of the nodes ( $\gamma \gg 1$ ) and an equivalent shortest path length ( $\lambda \approx 1$ ) compared with the random networks at both time points (pre test and post test). At the pretest, small-worldness ( $p = 0.0028$ ) was higher in the children with OB compared with HW controls, because of the higher normalized clustering coefficient ( $p = 0.0022$ ; see Fig. 3a). These between-group differences remained significant across different group thresholds ( $p_{\text{AUC}} = 0.002$ ;

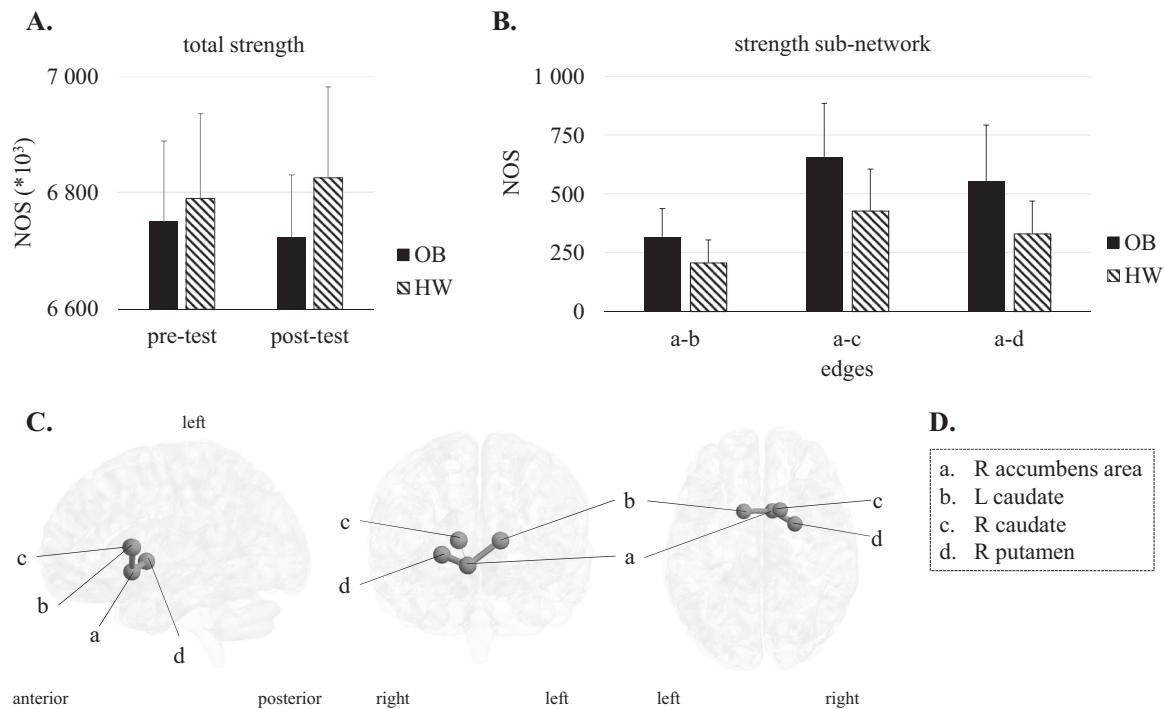


**Fig. 2** Overview of the results obtained by the network-based statistics (NBS) [26]. Bar graphs represent **a** the total number of reconstructed streamlines (NOS) between children with obesity (OB) and healthy weight (HW) controls across time points, and **b** the edge-specific NOS of the marginally higher connected subnetwork in children with OB

compared with HW controls. **c** Sagittal and axial views of the higher connected subnetwork in children with OB. Sphere size represents the nodes of the subnetwork and edge size represents the *t*-statistics magnitude, ranging from 3 to 3.7. **d** Table containing the names of the different nodes included in the subnetwork (L = left; R = right)

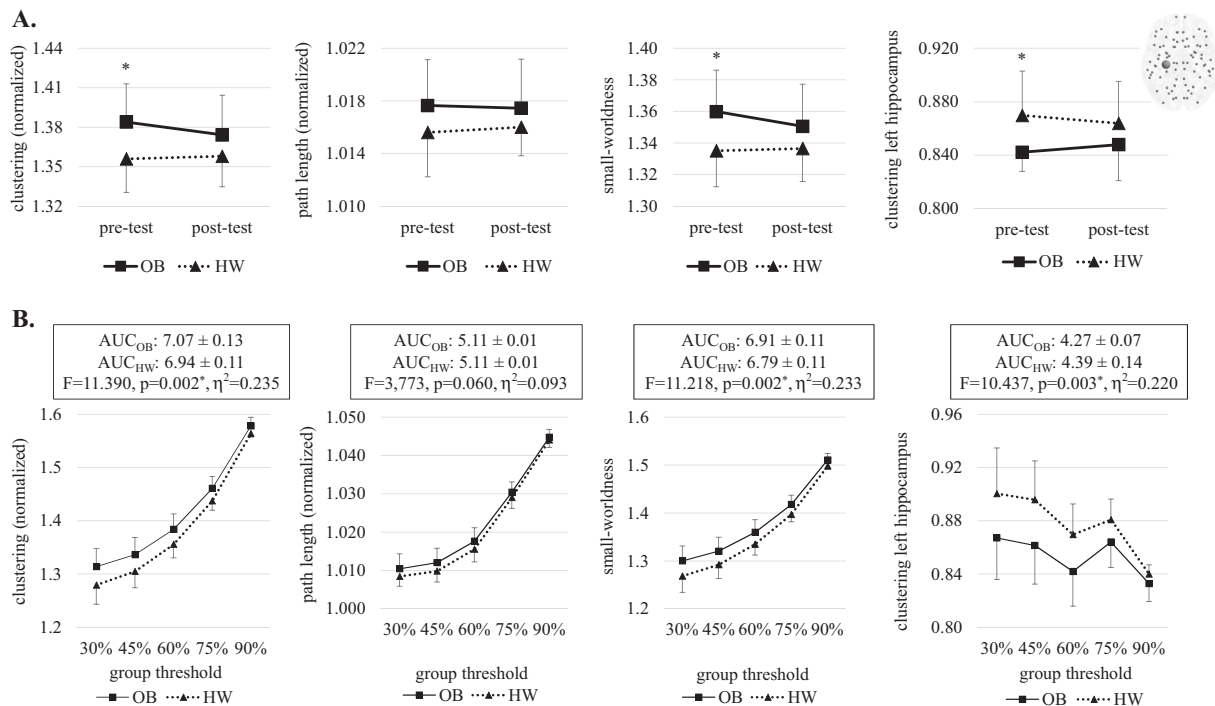


**Fig. 3** The **a** panel represents time (pre test vs. post test) by group (obesity (OB) vs. healthy weight (HW)) interaction effects of the global and regional graph analyses. The **b** panel shows group differences in graph metrics between children with OB and HW controls at the pretest across different group thresholds (30–90%, interval of 15%)

by calculating the area under the curve (AUC). Results of the one-way ANCOVAs, with age as a covariate, are presented (mean ± standard deviation, *F*, *p*, and eta squared ( $\eta^2$ )). Significant group differences at the pretest are represented by an asterisk ( $p < 0.05$ , FDR corrected)

see Fig. 3b). No differences were observed for normalized path length ( $p = 0.2318$ ). The results of the longitudinal plugin of the GAT toolbox revealed no significant time by group interaction effects ( $p > 0.05$ ). In other words, the differences in graph metrics between both groups did not change after OB treatment. The analyses were repeated with sex as a fixed factor. No significant group by sex interaction effects was observed. We can tentatively conclude that sex did not significantly influence the observed group differences in structural connectivity.

### Regional network properties

At the pretest, a significantly reduced clustering coefficient of the left hippocampus was observed in children with OB compared with HW controls ( $p = 0.0168$ , FDR corrected; see Fig. 3a). The clustering coefficient in this node remained significant for the other group thresholds ( $p_{AUC} = 0.003$ ; see Fig. 3b). The longitudinal analysis did not reveal significant time by group interaction effects for the clustering coefficient at the nodal level ( $p > 0.05$ , FDR corrected). The analyses were repeated with sex as a fixed factor. No significant group by sex interaction effects was observed. We can tentatively conclude that sex did not significantly influence the observed group differences in structural connectivity.

### Hubs

The hub network analyses revealed that both groups exhibited hubs at the pretest. Specifically, increased betweenness centrality (i.e., mean + two standard

deviations) was observed in the bilateral superior frontal gyrus and the right lateral orbitofrontal cortex. In addition, two regions, including the left lateral orbitofrontal cortex and the left precentral gyrus, could be identified as hubs in the children with OB but not in the HW controls. These results indicate a different hub distribution at the pretest in children with OB compared with HW controls.

### Changes in weight-related measures

The repeated measures ANOVA showed significant time by group interaction effects for body weight, percentage of body fat, waist circumference, and BMI ( $p$ 's  $\leq 0.001$ ). Post hoc analysis revealed a significant decrease in each of the weight-related measures in children with OB ( $p \leq 0.001$ ) after the program. In the HW control group, no significant changes in these measures ( $p > 0.05$ ) were observed between the pre test and post test, except for a small increase in body weight ( $p = 0.005$ ). Children with OB lost, on average, 18.8% ( $\pm 4.4\%$ ) of their baseline BMI and 5 out of 18 children could be identified as overweight instead of obese after the intervention.

### Partial correlations

No significant correlations were observed between (changes in) graph metrics or total strength and (changes in) anthropometric measurements ( $p > 0.05$ ; FDR corrected). Using an exploratory uncorrected threshold of  $p < 0.05$  [37], significant positive correlations were observed between graph metrics and weight-related measures at the pretest (see Fig. 4). Specifically, in the group of children with OB,

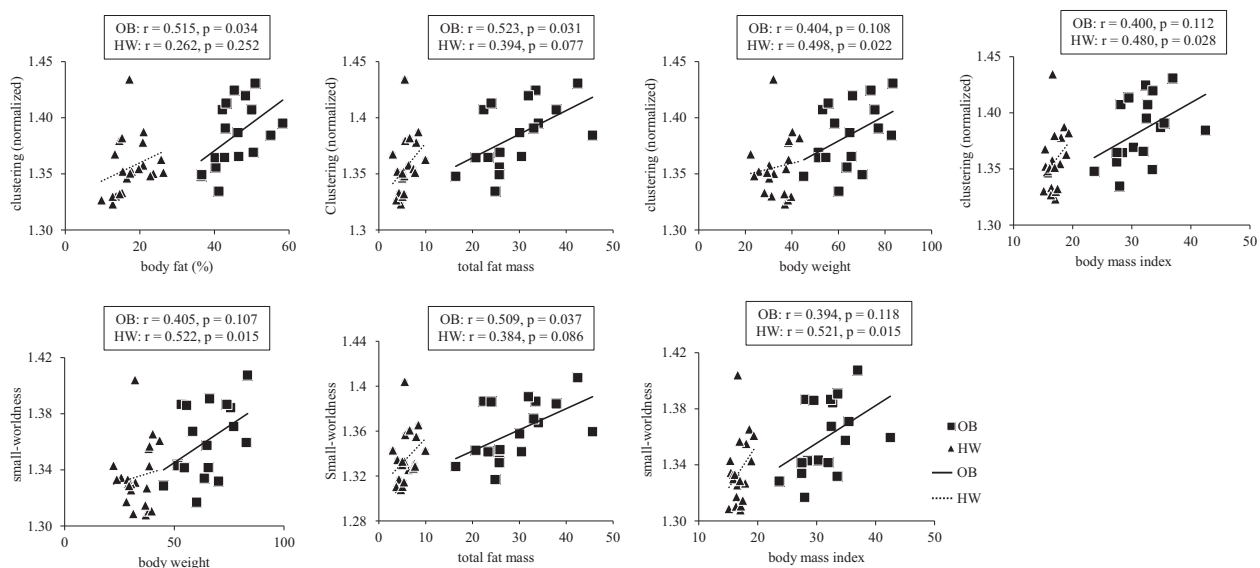


**Fig. 4** Scatterplots showing the partial correlations between graph metrics and weight-related measures in children with obesity (OB) compared with healthy weight (HW) controls at the pretest. The results

are uncorrected (i.e.,  $p < 0.05$ ). It is important to note that the correlation coefficients represented are based on partial correlations, corrected for age



a higher percentage of body fat at the start of the program was associated with higher network segregation (i.e., normalized clustering coefficient;  $r = 0.515$ ,  $p = 0.034$ ). In addition, higher total fat mass was associated with a higher normalized clustering coefficient ( $r = 0.523$ ,  $p = 0.031$ ) and small-worldness ( $r = 0.509$ ,  $p = 0.037$ ). In children with a HW, a higher body weight and BMI at the pretest were associated with a higher normalized clustering coefficient ( $r$ 's: 0.480–0.498;  $p$ 's: 0.028–0.022) and higher small-worldness ( $r$ 's: 0.522–0.521;  $p$ 's: 0.015–0.015). Since an outlier was detected for a normalized clustering coefficient and higher small-worldness in the HW control group (see Fig. 4), the analyses were repeated without this outlier. The previously observed positive correlations between a normalized clustering coefficient/small-worldness and body weight/BMI remained significant ( $r$ 's: 0.461–0.614;  $p$ 's: 0.004–0.041), except for the correlation between a normalized clustering coefficient and body weight ( $r = 0.403$ ,  $p = 0.078$ ).

## Discussion

To the best of our knowledge, this is the first study exploring differences between the structural connectomes of children with OB and those of HW controls using a GAT and NBS approach. Our results demonstrated an altered whole-brain network organization in children with OB compared with HW controls. Moreover, regional analyses revealed that regions and pathways of the motor cortex and reward network were affected in children with OB. No changes were observed in their structural connectomes after following a standard 5-month multidisciplinary OB treatment program.

Global network analyses revealed that both groups (OB and HW) exhibited a small-world organization, reflecting an optimal balance between local segregation and global integration [14]. The structural connectomes of children with OB, however, showed a significantly higher normalized clustering coefficient compared with the HW controls. Moreover, partial correlations showed that a higher BMI was significantly associated with a more segregated brain network in the HW controls, albeit using an uncorrected  $p$ -value ( $p < 0.05$ ). Overall, these findings suggest that the structural connectomes of children with a higher BMI are more segregated into local clusters of connections. Previous neuroimaging studies reported a reduced normalized clustering coefficient in adolescents and adults with OB compared with HW controls [18–20], whereby the majority of participants reached the pubertal stage. The different findings between child and adult studies may be due to the effects of brain maturation [38, 39]. Studies in the field of growth connectomics reported that brain networks mature

from a “local” to a more “distributed” network organization during late childhood (7–11 years) [40]. This process is characterized by a decrease in local segregation and an increase in global integration [38]. In addition, previous network studies have shown that children with developmental disorders, such as attention-deficit hyperactivity disorder and autism spectrum disorder, have higher local segregation compared with typically developing children [41–43]. Thus, our results may suggest delayed network development in children with OB compared with HW controls, even though no significant group differences in pubertal status were observed.

The hub network analyses revealed an increased central role of key frontal regions in children with OB. Although hubs were identified in both groups, a difference in the distribution of hub regions with high betweenness centrality was observed between children with OB and HW controls. Specifically, the left precentral gyrus and the left orbito-frontal cortex acted as hubs in the children with OB but not in the HW controls. The precentral gyrus, corresponding to the primary motor cortex (BA4), receives sensory-motor information from (sub-)cortical brain regions and sends this information to lower body parts. Thus, this region plays an important role in controlling the execution of movements [44]. Our recent studies have shown that childhood OB is associated with reduced gross and fine motor skills [45–47], which hampers their successful participation in physical activities [4]. Moreover, neuroimaging studies have suggested that these motor deficits in children with OB are accompanied with gray and white matter alterations in motor-related regions in the brain [8, 10]. Since hub regions are thought to play a crucial role in the coordination of information flow [48], the increased importance of the left precentral gyrus in children with OB may be related to their reduced motor skills. However, further research is needed to understand the precise biophysical processes underlying this potential association.

The other hub region found in the OB group but not in the HW group was the left lateral orbitofrontal cortex. This region receives connections from parts of the limbic system and sensory modalities, and is involved in behavior-related decision-making (e.g., choice between healthy and unhealthy food, or active and inactive behavior) [49]. Moreover, this region has shown to be a key structure in the reward network, which is a subnetwork in the brain that is responsible for the hedonic (“liking”) or incentive (“wanting”) salience of behavior [20, 50]. Interestingly, the regional network analyses using both approaches (GAT and NBS) strengthened this result, with altered local segregation and structural network strength, mainly in regions and pathways of the reward system. Specifically, children with OB demonstrated lower nodal clustering in the hippocampus and higher structural network strength of edges

connecting regions of the striatum. Moreover, previous studies using structural or task-related functional MRI have suggested that excessive eating behavior and/or physical inactivity in children and adolescents with OB is associated with alterations in the reward network [6, 9, 51–53]. Human behavior often involves decision-making, such as choosing between healthy and unhealthy foods or between physical activities and sedentary behaviors [8, 20, 37]. These choices can be driven by reward-seeking processes (“drive”) or executive functions (“control”) [37]. Reward-seeking processes are responsible for automatic, impulsive decisions driven in favor of perceived immediate rewards (e.g., feelings, taste, and aroma) and are regulated by limbic and paralimbic brain regions. Since these reward-seeking processes often drive choices that may have negative health consequences, executive functions are needed to override automatic, impulsive responses in order to make health-related decisions [54]. Executive functions facilitate goal-directed behavior (e.g., being more physically active) by suppressing impulsive responses (e.g., watching a movie), changing habits (e.g., sedentary behavior), or planning (future) behaviors in new or changing situations (e.g., learning a new motor skill) [5]. This control system is regulated by the prefrontal cortex, which is among the last brain regions to mature (i.e., mid-1920s [55–57]). Given that limbic brain regions mature in an earlier stage of development, children and adolescents are particularly susceptible to make unhealthy, reward-driven decisions, especially in the current “obesogenic” environment that fosters unhealthy eating behavior and sedentary behavior. In this respect, it might be that children with OB, who have reduced structural connectivity in the reward network, are more likely to choose for rewarding, but unhealthy, behaviors (e.g., physical inactivity, sedentary behavior, excess, and high-caloric food intake) compared with children with an adequate level of cognitive control, which in turn increases their risk of developing OB. Taken together, our findings suggest that the brain structure of the reward network is affected in children with OB, which further emphasizes the role of the reward system in this multifactorial health problem.

Consistent with previous research, the multidisciplinary OB program resulted in a considerable amount of weight loss ( $\Delta 17.9$ – $21.7\%$ ) [28, 29]. Although this program has shown to increase levels of physical activity [58], enhance healthy eating habits [59], and induce local changes in brain structure [11], no significant training-induced changes in the structural connectomes of children with OB were observed after a period of 5 months. These findings indicate that a multidisciplinary OB program consisting of diet restriction, cognitive behavioral therapy, and physical activity has no immediate impact on the structural network organization of children with OB. The absence of significant alterations

after treatment in this study may be due to several factors. First, it could be that the observed differences at baseline relate to genetic factors that are not amenable to behavioral intervention. High heritability estimates (ranging from 21% to 82%) have been observed for network organization, particularly in the cerebellum (79–82%) and subcortical structures, including the putamen (71%) and accumbens area (65%), which both showed increased structural network strength in children with OB compared with HW peers [60]. Second, the treatment duration may have been insufficient to induce network-level changes in the brain. Alternatively, neuroplasticity could conceivably be delayed for weeks or months post treatment. Thus, follow-up studies are needed to serially test neural responses and long-term network effects following treatment [37, 61]. Third, the absence of significant alterations could simply reflect a lack of power, due to the relatively small sample size. Therefore, future longitudinal studies with larger data sets could further elucidate the impact of treatment on children’s brain structure.

This study has some limitations that need to be addressed. First, data of developmental and/or medical factors (such as number of years being obese, physical activity, socioeconomic status, and comorbidities) were lacking, and therefore, it was not possible to control for these potential confounders. Second, the structural connectomes of children with OB who followed a multidisciplinary OB program were compared with those of HW controls who were not involved in any kind of treatment. It would be interesting to compare this intervention group with a control group of children with OB who are not involved in a specific treatment program. This would make it a randomized controlled trial, instead of a pre-experimental study, on the assumption that children with OB are randomly assigned to either the intervention or the control group. Third, due to the absence of a field map or a reverse-phase encoding image, it was not possible to correct for EPI distortions during the preprocessing of the DWI images. To be comprehensive, scans were visually inspected for artifacts, during which DWI scans were removed from the analysis (four OB, one HW) due to poor image quality (movement artifacts, ghosting, and signal drops). Finally, the results of the partial correlations were interpreted using an exploratory uncorrected threshold of  $p < 0.05$ . Although reporting these results is important to help motivate future studies, interpretation of these results should be done with caution [37].

Despite these limitations, this is the first study that provides evidence for an affected global network organization in children with OB compared with HW controls. Moreover, regional analyses revealed significant alterations in local segregation and structural network strength of brain regions and connections involved in motor and reward control, suggesting that these brain regions play an

important role in this multifactorial health problem and related behaviors. Although we did not examine children's motor and reward control directly in this study, our findings suggest that clinicians should not only focus on weight loss, but also improve children's motor competence and executive functioning, which is in line with previous studies [9, 11, 52]. Finally, the absence of significant alterations in the structural connectome of children with OB after a 5-month multidisciplinary OB program may call for larger data sets to examine the impact of short-term and long-term weight loss on children's brain network organization.

**Acknowledgements** The study was funded by the Ph.D. fellowship of the Research Foundation Flanders (FWO) awarded to MJCMA [3F000714]. The authors are very grateful to all participants and their parents, the staff from the rehabilitation center "Zeepreventorium" (De Haan, Belgium), and the board of the participating schools.

**Funding** This study was funded by the Ph.D. fellowship of the Research Foundation Flanders (FWO) awarded to MJCMA [3F000714].

**Author contributions** Conception and design of the experiment: MJCMA, FJAD, ED'H, ML, and KC. Collection and processing of the data: MJCMA, LVA, MADB, and AZ. Interpretation of the results: MJCMA, MADB, FJAD, ED'H, ML, KC, and AZ. Drafting of the paper and critical revision: MJCMA, MADB, FJAD, ED'H, ML, KC, AZ, ADG, and LVA. All authors had final approval of the submitted and published version.

## Compliance with ethical standards

**Conflict of interest** The authors declare that they have no conflict of interest.

**Publisher's note:** Springer Nature remains neutral with regard to jurisdictional claims in published maps and institutional affiliations.


## References

- Sahoo K, Sahoo B, Choudhury AK, Sufi NY, Kumar R, Bhadoria AS. Childhood obesity: causes and consequences. *J Fam Med Prim Care*. 2015;4:187–92.
- Keating CL, Moodie ML, Swinburn BA. The health-related quality of life of overweight and obese adolescents – a study measuring body mass index and adolescent-reported perceptions. *Int J Pediatr Obes*. 2011;6:434–41.
- Wijnhoven TM, van Raaij JM, Yngve A, Sjöberg A, Kunešová M, Duleva V, et al. WHO European Childhood Obesity Surveillance Initiative: health-risk behaviours on nutrition and physical activity in 6–9-year-old school children. *Public Health Nutr*. 2015;18:3108–24.
- Robinson LE, Stodden DF, Barnett LM, Lopes VP, Logan SW, Rodrigues LP, et al. Motor competence and its effect on positive developmental trajectories of health. *Sport Med*. 2015;45:1273–84.
- Joseph RJ, Alonso-Alonso M, Bond DS, Pascual-Leone A, Blackburn GL. The neurocognitive connection between physical activity and eating behaviour. *Obes Rev*. 2011;12:800–12.
- Liang J, Matheson BE, Kaye WH, Boutelle KN. Neurocognitive correlates of obesity and obesity-related behaviors in children and adolescents. *Int J Obes*. 2014;38:494–506.
- Hansen CJ, Stevens LC, Coast JR. Exercise duration and mood state: how much is enough to feel better? *Heal Psychol*. 2001;20:267–75.
- Ou X, Andres A, Pivik RT, Cleves MA, Badger TM. Brain gray and white matter differences in healthy normal weight and obese children. *J Magn Reson Imaging*. 2015;42:1205–13.
- Moreno-López L, Soriano-Mas C, Delgado-Rico E, Rio-Valle JS, Verdejo-García A. Brain structural correlates of reward sensitivity and impulsivity in adolescents with normal and excess weight. *PLoS ONE*. 2012;7:e49185.
- Augustijn MJCMA, Deconinck FJA, D'Hondt E, Van Acker L, De Guchteneere A, Lenoir M, et al. Reduced motor competence in children with obesity is associated with structural differences in the cerebellar peduncles. *Brain Imaging Behav*. 2018;12:1000–10.
- MJCMA Augustijn, D'Hondt E, Leemans A, Van Acker L, De Guchteneere A, Lenoir M, et al. Weight loss, behavioural change and structural neuroplasticity in children with obesity through a multidisciplinary treatment program. *Hum Brain Mapp*. 2018;12:1000–10.
- Bressler SL, Menon V. Large-scale brain networks in cognition: emerging methods and principles. *Trends Cogn Sci*. 2010;14:277–90.
- Rubinov M, Sporns O. Complex network measures of brain connectivity: uses and interpretations. *Neuroimage*. 2010;52:1059–69.
- Bassett DS, Bullmore E. Small-world brain networks. *Neuroscientist*. 2006;12:512–23.
- Bruce AS, Martin LE, Savage CR. Neural correlates of pediatric obesity. *Prev Med*. 2011;52:S29–35.
- Sporns O, Tononi G, Kötter R. The human connectome: a structural description of the human brain. *PLoS Comput Biol*. 2005;1:0245–51.
- Griffa A, Baumann PS, Thiran JP, Hagmann P. Structural connectomics in brain diseases. *Neuroimage*. 2013;80:515–26.
- Chao S-H, Liao Y-T, Chen VC-H, Li C-J, McIntyre RS, Lee Y, et al. Correlation between brain circuit segregation and obesity. *Behav Brain Res*. 2018;337:218–27.
- Baek K, Morris LS, Kundu P, Voon V. Disrupted resting-state brain network properties in obesity: decreased global and putaminal cortico-striatal network efficiency. *Psychol Med*. 2017;47:585–96.
- Marqués-Iturria I, Scholtens LH, Garolera M, Pueyo R, García-García I, González-Tartiere P, et al. Affected connectivity organization of the reward system structure in obesity. *Neuroimage*. 2015;111:100–6.
- Yuan W, Treble-Barna A, Sohlberg MM, Harn B, Wade SL. Changes in structural connectivity following a cognitive intervention in children with traumatic brain injury. *Neurorehabil Neural Repair*. 2017;31:190–201.
- Yuan W, Wade SL, Quatman-Yates C, Hugentobler JA, Gubanich PJ, Kurowski BG. Structural connectivity related to persistent symptoms after mild tbi in adolescents and response to aerobic training: preliminary investigation. *J Head Trauma Rehabil*. 2017;32:378–84.
- Amidi A, Hosseini SMH, Leemans A, Kesler SR, Agerbæk M, Wu LM, et al. Changes in brain structural networks and cognitive functions in testicular cancer patients receiving cisplatin-based chemotherapy. *J Natl Cancer Inst*. 2017;109:1–7.
- Langer N, von Bastian CC, Wirz H, Oberauer K, Jäncke L. The effects of working memory training on functional brain network efficiency. *Cortex*. 2013;49:2424–38.
- Caeyenberghs K, Metzler-Baddeley C, Foley S, Jones DK. Dynamics of the human structural connectome underlying working memory training. *J Neurosci*. 2016;36:4056–66.

26. Zalesky A, Fornito A, Bullmore ET. Network-based statistic: identifying differences in brain networks. *Neuroimage*. 2010;53:1197–207.
27. Cole TJ, Lobstein T. Extended international (IOTF) body mass index cut-offs for thinness, overweight and obesity. *Pediatr Obes*. 2012;7:284–94.
28. D'Hondt E, Gentier I, Deforche B, Tanghe A, De Bourdeaudhuij I, Lenoir M. Weight loss and improved gross motor coordination in children as a result of multidisciplinary residential obesity treatment. *Obesity*. 2011;19:1999–2005.
29. Gentier I, D'Hondt E, Augustijn M, Tanghe A, De Bourdeaudhuij I, Deforche B, et al. Multidisciplinary residential treatment can improve perceptual-motor function in obese children. *Acta Paediatr*. 2015;104:e263–70.
30. Goscinski WJ, McIntosh P, Felzmann U, Maksimenko A, Hall CJ, Gureyev T, et al. The Multi-modal Australian ScienceS Imaging and Visualization Environment (MASSIVE) high performance computing infrastructure: applications in neuroscience and neuroinformatics research. *Front Neuroinform*. 2014;8:1–13.
31. Roberts JA, Perry A, Lord AR, Roberts G, Mitchell PB, Smith RE, et al. The contribution of geometry to the human connectome. *Neuroimage*. 2016;124:379–93.
32. Zalesky A, Fornito A, Cocchi L, Gollo LL, van den Heuvel MP, Breakspear M. Connectome sensitivity or specificity: which is more important? *Neuroimage*. 2016;142:407–20.
33. Kaiser M, Hilgetag CC. Nonoptimal component placement, but short processing paths, due to long-distance projections in neural systems. *PLoS Comput Biol*. 2006;2:e0805–15.
34. Hosseini SMH, Hoefft F, Kesler SR, Lambiotte R. GAT: a graph-theoretical analysis toolbox for analyzing between-group differences in large-scale structural and functional brain networks. *PLoS ONE*. 2012;7:e40709.
35. De Reus MA, Van Den Heuvel MP. Estimating false positives and negatives in brain networks. *Neuroimage*. 2013;70:402–9.
36. Marshall WA, Tanner JM. Variations in the pattern of pubertal changes in boys. *Arch Dis Child*. 1970;45:13–23.
37. Caeyenberghs K, Clemente A, Imms P, Egan G, Hocking DR, Leemans A, et al. Evidence for training-dependent structural neuroplasticity in brain-injured patients: a critical review. *Neurorehabil Neural Repair*. 2018;32:99–114.
38. Hagmann P, Sporns O, Madan N, Cammoun L, Pienaar R, Wedeen VJ, et al. White matter maturation reshapes structural connectivity in the late developing human brain. *Proc Natl Acad Sci USA*. 2010;107:19067–72.
39. Collin G, Van Den Heuvel MP. The ontogeny of the human connectome: Development and dynamic changes of brain connectivity across the life span. *Neuroscientist*. 2013;19:616–28.
40. Fair DA, Cohen AL, Power JD, Dosenbach NUF, Church JA, Miezin FM, et al. Functional brain networks develop from a “Local to Distributed” organization. *PLoS Comput Biol*. 2009;5:e1000381.
41. Wang L, Zhu C, He Y, Zang Y, Cao Q, Zhang H, et al. Altered small-world brain functional networks in children with attention-deficit/hyperactivity disorder. *Hum Brain Mapp*. 2009;30:638–49.
42. Di Martino A, Fair DA, Kelly C, Satterthwaite TD, Castellanos FX, Thomason ME, et al. Unraveling the miswired connectome: a developmental perspective. *Neuron*. 2014;83:1335–53.
43. Caeyenberghs K, Taymans T, Wilson PH, Vanderstraeten G, Hosseini H, van Waelvelde H. Neural signature of developmental coordination disorder in the structural connectome independent of comorbid autism. *Dev Sci*. 2016;19:599–612.
44. Rizzolatti G, Luppino G. The cortical motor system. *Neuron*. 2001;31:889–901.
45. D'Hondt E, Deforche B, De Bourdeaudhuij I, Lenoir M. Childhood obesity affects fine motor skill performance under different postural constraints. *Neurosci Lett*. 2008;440:72–5.
46. D'Hondt E, Deforche B, De Bourdeaudhuij I, Lenoir M. Relationship between motor skill and body mass index in 5- to 10-year-old children. *Adapt Phys Activ Q*. 2009;26:21–37.
47. Gentier I, D'Hondt E, Shultz S, Deforche B, Augustijn M, Hoorne S, et al. Fine and gross motor skills differ between healthy-weight and obese children. *Res Dev Disabil*. 2013;34:4043–51.
48. Sporns O, Honey CJ, Kötter R. Identification and classification of hubs in brain networks. *PLoS ONE*. 2007;2:e1049.
49. Rudebeck PH, Murray EA. The orbitofrontal oracle: cortical mechanisms for the prediction and evaluation of specific behavioral outcomes. *Neuron*. 2014;84:1143–56.
50. Volkow ND, Wang G-J, Baler RD. Reward, dopamine and the control of food intake: implications for obesity. *Trends Cogn Sci*. 2011;15:37–46.
51. van den Berg L, Pieterse K, Malik JA, Luman M, Willems van Dijk K, Oosterlaan J, et al. Association between impulsivity, reward responsiveness and body mass index in children. *Int J Obes*. 2011;35:1301–7.
52. Verdejo-García A, Verdejo-Román J, Rio-Valle JS, Lacomba JA, Lagos FM, Soriano-Mas C. Dysfunctional involvement of emotion and reward brain regions on social decision making in excess weight adolescents. *Hum Brain Mapp*. 2015;36:226–37.
53. Kravitz AV, O'Neal TJ, Friend DM. Do dopaminergic impairments underlie physical inactivity in people with obesity? *Front Hum Neurosci*. 2016;10:1–8. (514)
54. Diamond A. Executive functions. *Annu Rev Psychol*. 2013;64:135–68.
55. Casey BJ, Giedd JN, Thomas KM. Structural and functional brain development and its relation to cognitive development. *Biol Psychol*. 2000;54:241–57.
56. Gogtay N, Giedd JN, Lusk L, Hayashi KM, Greenstein D, Vaituzis A C, et al. Dynamic mapping of human cortical development during childhood through early adulthood. *Proc Natl Acad Sci USA*. 2004;101:8174–9.
57. Willoughby T, Good M, Adachi PJC, Hamza C, Tavernier R. Examining the link between adolescent brain development and risk taking from a social-developmental perspective. *Brain Cogn*. 2014;89:70–8.
58. Deforche B, De Bourdeaudhuij I, Debode P, Vinaimont F, Hills AP, Verstraete S, et al. Changes in fat mass, fat-free mass and aerobic fitness in severely obese children and adolescents following a residential treatment programme. *Eur J Pediatr*. 2003;162:616–22.
59. Braet C, Tanghe A, Decaluwé V, Moens E, Rosseel Y. Inpatient treatment for children with obesity: weight loss, psychological well-being, and eating behavior. *J Pediatr Psychol*. 2004;29:519–29.
60. Weise CM, Thiyyagura P, Reiman EM, Chen K, Krakoff J. Fat-free body mass but not fat mass is associated with reduced gray matter volume of cortical brain regions implicated in autonomic and homeostatic regulation. *Neuroimage*. 2013;64:712–21.
61. Thomas C, Baker CI. Teaching an adult brain new tricks: a critical review of evidence for training-dependent structural plasticity in humans. *Neuroimage*. 2013;73:225–36.
62. Jenkinson M, Beckmann CF, Behrens TEJ, Woolrich MW, Smith SM. FSL. *Neuroimage*. 2012;62:782–90.
63. Tournier J-DD, Calamante F, Connelly A. MRtrix: diffusion tractography in crossing fiber regions. *Int J Imaging Syst Technol*. 2012;22:53–66.

64. Desikan RS, Ségonne F, Fischl B, Quinn BT, Dickerson BC, Blacker D, et al. An automated labeling system for subdividing the human cerebral cortex on MRI scans into gyral based regions of interest. *Neuroimage*. 2006;31:968–80.

## Affiliations

Mireille J. C. M. Augustijn <sup>1,2</sup> · Maria A. Di Biase<sup>3,4,5</sup> · Andrew Zalesky<sup>3,4,6</sup> · Lore Van Acker<sup>7</sup> · Ann De Guchtenaere<sup>7</sup> · Eva D'Hondt<sup>8</sup> · Matthieu Lenoir<sup>1</sup> · Frederik J. A. Deconinck<sup>1</sup> · Karen Caeyenberghs<sup>9</sup>

<sup>1</sup> Department of Movement and Sports Sciences, Ghent University, Watersportlaan 2, 9000 Gent, Belgium

<sup>2</sup> Research Foundation Flanders (FWO), Melbourne Neuropsychiatry Centre, The University of Melbourne and Melbourne Health, Carlton South, VIC, Australia

<sup>3</sup> Department of Psychiatry, Melbourne Neuropsychiatry Centre, The University of Melbourne and Melbourne Health, Carlton South, VIC, Australia

<sup>4</sup> Department of Psychiatry, The University of Melbourne, Parkville, VIC, Australia

<sup>5</sup> Psychiatry Neuroimaging Laboratory, Brigham and Women's

Hospital, Harvard Medical School, Boston, MA, USA

<sup>6</sup> Melbourne School of Engineering, The University of Melbourne, Parkville, VIC, Australia

<sup>7</sup> Zeepreventorium VZW, Koninklijke Baan 5, 8420 De Haan, Belgium

<sup>8</sup> Faculty of Physical Education and Physiotherapy, Department of Movement and Sports Sciences, Vrije Universiteit Brussel, Pleinlaan 2, 1050 Brussel, Belgium

<sup>9</sup> School of Psychology, Australian Catholic University, 115 Victoria Pde, Melbourne, VIC 3065, Australia